p-doping of organic hole transport layers in p-i-n perovskite solar cells: correlating open-circuit voltage and photoluminescence quenching

Tian Du,[1,2†] Weidong Xu,[2†] Matyas Daboczi,[3] Jinhyun Kim,[2] Shengda Xu,[1] Chieh-Ting Lin,[1,2] Hongkyu Kang,[3,4] Kwanghee Lee,[4] Martin J. Heeney[2], Ji-Seon Kim[3], James R. Durrant[2,5,*] and Martyn A. McLachlan[1,*]

[1]*Department of Materials and Centre for Plastic Electronics, Imperial College, London, SW7 2AZ, United Kingdom*
[2]*Department of Chemistry and Centre for Plastic Electronics, Imperial College, London, SW7 2AZ, United Kingdom*
[3]*Department of Physics and Centre for Plastic Electronics, Imperial College, London, SW7 2AZ, United Kingdom*
[4]*Research Institute for Solar and Sustainable Energies, Gwangju Institute of Science and Technology, Gwangju 61005, Republic of Korea*
[5]*SPECIFIC IKC, College of Engineering, Swansea University, SA2 7AX, United Kingdom*

[†]*These authors contributed equally to this work*

Supporting Information

Experimental details

Device fabrication and measurement. All devices were fabricated on indium-doped tin oxide (ITO) glass, a transparent conducting substrate. The substrates were sequentially cleaned in ultrasonic bath in acetone, isopropanol and deionized water for 10 minutes, respectively, and were dried under nitrogen flow. Prior to deposition of hole transport layers, all ITO substrates were treated by oxygen plasma for 10 minutes. PTPD and PTAA (0.25wt. % in chlorobenzene for all) were spin-coated onto ITO substrates at 5000 rpm for 20s. After drying for 1 minute, PFN (0.05wt. % in methanol) was spin-coated onto PTPD and PTAA layer at 5000 rpm for 20s. PTPD and PFN were received from 1 Materials LTD, the PTAA was synthesized in-house. For the other device, PEDOT:PSS was spin-coated on ITO substrates at 4000 rpm for 45 seconds, and were subsequently annealed at 150 °C for 15 minutes. All depositions were performed in ambient condition, and the substrates were transferred into a nitrogen-filled glovebox afterwards.

$CH_3NH_3PbI_3$ (MAPI) perovskite precursor solution was prepared by dissolving 1.5 M lead iodide (PbI_2, 99.985%) and methylammonium iodide (MAI) of equal molar ratio in a mixture solvent of N,N-Dimethylmethanamide (DMF) and Dimethyl sulfoxide (DMSO) (9:1.1 in volume). The solution was stirred at 50°C for 1h to fully dissolve the precursors and was infiltrated with 0.45 µm filter before use. 40 µl precursor solution was dropped onto substrates with hole transport layers and was spun at 4000 rpm for 30s. At 7th second, 0.5 ml diethyl ether was instantly dripped onto the spinning substrate. The substrates were then annealed on a hot plate at 100°C for 15 minutes.

Solution electron transport materials was prepared by dissolving 23 mg/ml Phenyl-C61-butyricacid methylester (C60-PCBM) in chlorobenzene. The solution was stirred at 40 °C for 1h and was infiltrated with 0.45 µm filter before use. PCBM solution was spin-coated on MAPI film at 2000 rpm for 45 seconds. Finally, the devices were completed by thermally evaporating 0.7 nm of lithium fluoride (LiF) and 100 nm of Ag on PCBM layer under $5x10^{-6}$ mbar.

Current density-voltage (J-V) characteristics were measured with a Keithley 2400 source meter. The cells were illuminated by an AM 1.5 xenon lamp solar simulator (Oriel Instruments). The intensity was adjusted to 1 sun by changing the working current, which was calibrated using a Si reference

photodiode. All devices were stored in dark prior to measurement and were measured in a nitrogen-filled chamber. External quantum efficiency (EQE) spectra were measured with a PV Measurements QEX10 system. The spectral response was measured between 300 and 850 nm and was calibrated with a silicon reference photodiode.

Physical and morphological characterization. X-ray diffraction (XRD) patterns of perovskite films were obtained with a X'pert Powder diffractometer (PANalytical), Cu Kα source. The diffraction patterns were measured over the range 7 - 40° 2θ. The samples were rotated during measurement. The top-view and cross-sectional scanning electron microscopy (SEM) images were obtained using a LEO Gemini 1525 field emission gun scanning electron microscopy. The working voltage of SEM was fixed at 5 kV. To prevent charging, all the films were coated with 10 nm chromium layer.

Photoluminescence and absorption spectroscopy measurements. Photoluminescence spectroscopy of by-layer films and steady state 1-Sun PL of full devices were measured with a FL 1039 spectrometer (Horiba Scientific). Illumination is provided by a white light LED (B3590N) purchased from CREE with output wavelength from 400 nm to 700 nm, excitation density was calibrated to 1-Sun equivalent by monitoring the J_{SC} of the device. Two short pass filters with edge of 700nm were used before samples to cut off the unwanted light after 700 nm and two long pass filters after 700 nm were used before the detectors to avoid white light background.

Ultraviolet-visible (UV-Vis) absorption spectra were obtained with a Horriba UV-vis spectrophotometer by measuring both transmittance and reflectance spectra of the perovskite films, with step-size of 1nm and integrating time of 0.5s.

Photoelectron spectroscopy. An APS04 (KP Technology) system was used to determine the energy levels of the hole transport materials. The HOMO of the semiconductors was measured by Ambient Pressure Photoemission Spectroscopy (APS) technique. Fermi energy levels were determined by a vibrating tip (2 mm diameter, gold alloy) Kelvin probe after the samples reached equilibrium in dark. A cleaned silver reference measured before the samples by both Kelvin probe and APS was applied to calibrate the work function of the Kelvin probe tip.

Transient optoelectronic measurement All cells show approximate linear increase of J_{SC} with light intensity (**Figure S6**). The solar cells are held at certain level of V_{OC}s by varying background illumination intensities with white-light LED arrays. In addition to this, a small amount of excess charge, ΔQ, is created in the devices as a result of the pulsed laser perturbation, we then probe the resulting voltage change (TPV) ΔV ($<<V_{oc}$) and calculate the differential capacitance as

$$C_{DC}(V) = \frac{\Delta Q}{\Delta V}$$

The excess charge ΔQ is separately measured, with the device held at short circuit, by integrating the transient photocurrent (TPC) generated by the same optical perturbation. The capacitance as a function of V_{OC} is shown in **Figure S7**. Fitting the capacitance distribution with an exponential, the total excess

electronic charge, n [cm^{-2}], stored in the device at open circuit can be estimated by integration of the capacitance with respect to voltage after subtracting $C_{electrode}$:

$$n(V_{oc}) = \frac{1}{q}\int_0^{V_{oc}} C_{DC}(V) - C_{electrode} dV$$

the recombination rate of the small amount of excess charge generated by laser perturbation, τ, can be derived from decays of TPV transients that are measured at different background light intensities. **Figure S8** shows two representative TPV decays under dark condition and under 1-Sun equivalent illumination. Although a correction estimation of estimate recombination flux requires the small-perturbation lifetime to be converted to the pseudo-first-order lifetime of total excess charge carriers $\tau_n = \delta\tau$, by a reaction order of δ (see Ref 6 and Ref 7), this is not considered in this study and only the small perturbation lifetimes are compared between these devices.

The measurements of excess charge accumulated in the device coupled with the measured photovoltage decay time-constants can be used to reconstruct the measured V_{oc} to check internal consistency between the measurements. With the data of excess charge accumulated in the working device, and the measured photovoltage decay time-constants we should be able to calculate recombination current $J_{rec} = Q/\tau_n$. At open circuit recombination current should be equal and opposite to generation current that assumed to be $J_{SC.}$ Using only these measured data and their corresponding fitting parameters the reconstructed open circuit voltage, V_{oc}^{Rec}, can be found as

$$V_{oc}^{Rec} = \frac{mk_BT}{q\delta}\ln\left(\frac{\tau_{n,0}J_{SC}}{qn_0}\right)$$

where m, δ, $\tau_{n,0}$, n_0 are fitting parameters.

Supporting figures

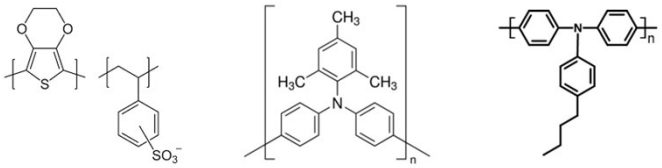

Figure S1 The chemical structures of organic hole transport materials.

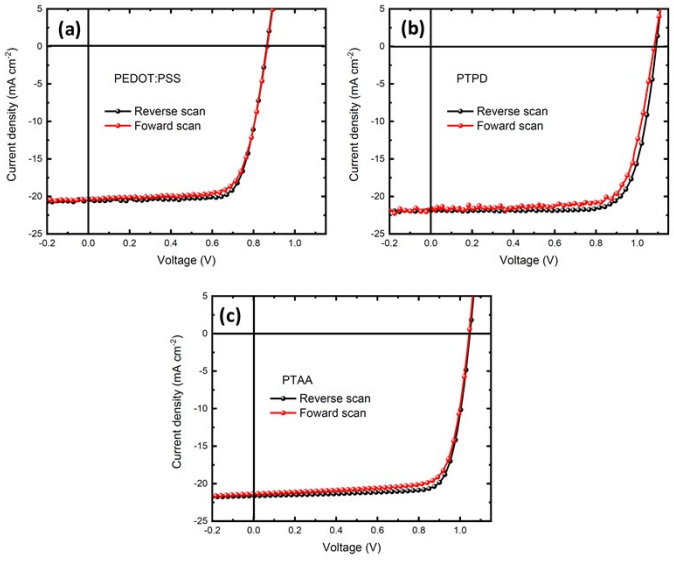

Figure S2 J-V scans showing the variation in hysteresis observed with the different HTLs.

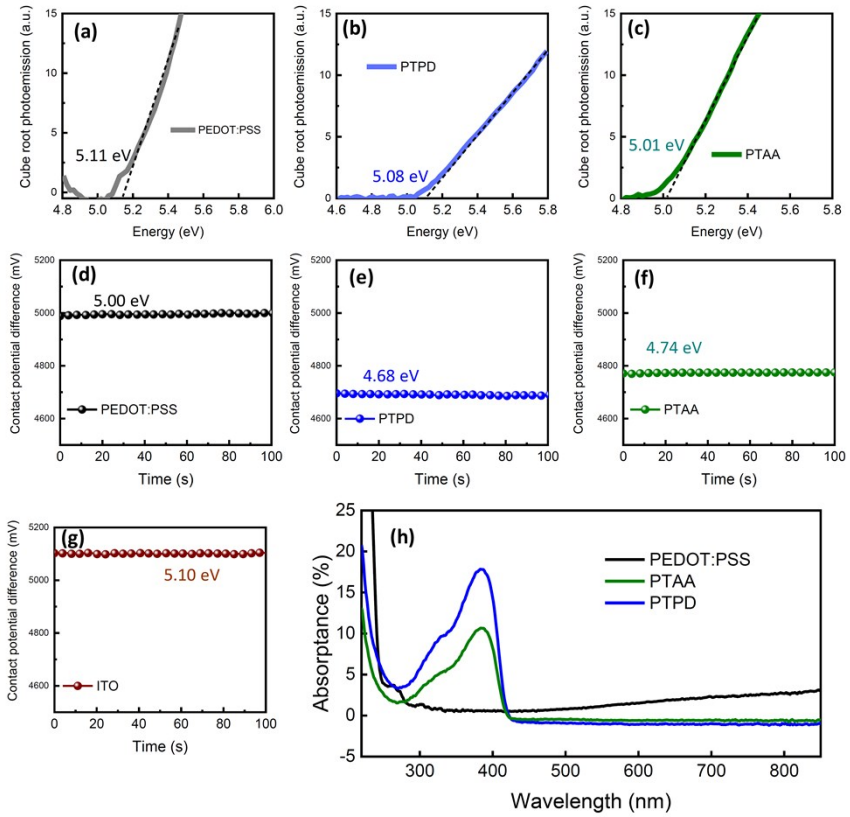

Figure S3 a) - c), Photoemission spectra of the hole transport layers (HTLs). **d) – g)** Work function of the HTLs and ITO. **h)** Absorptance spectra of the HTLs.

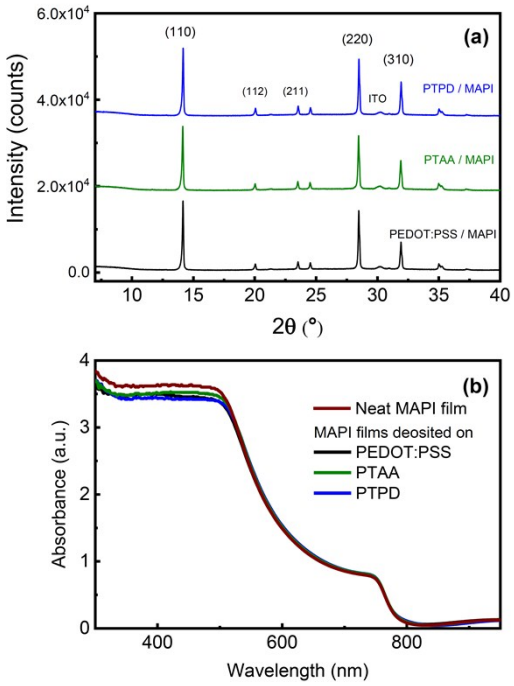

Figure S4 Properties of bulk perovskite deposited on different HTLs. **a)** X-ray diffraction patterns and **b)** ultraviolet-visible (UVvis) absorbance spectra.

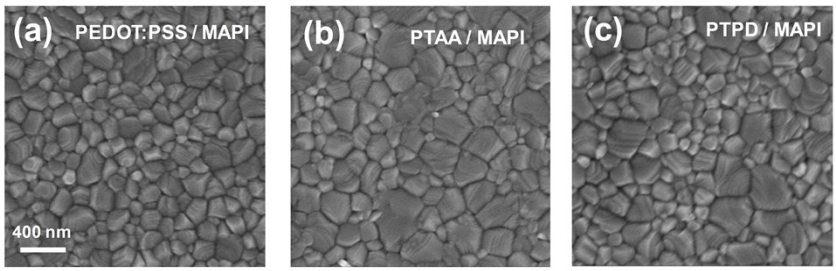

Figure S5 Surface scanning electron microscopy (SEM) images of MAPI films deposited on different HTLs.

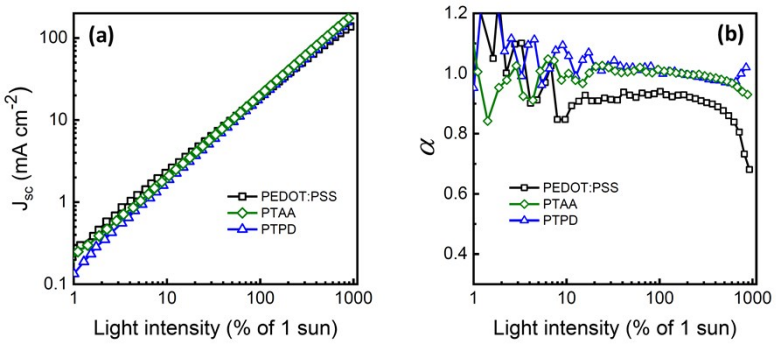

Figure S6 a) Short-circuit current density J_{SC} as a function of light intensity (I). **b)** Linearity of J_{SC} (α) against light intensity derived from a relationship of $J_{sc} \propto I^{\alpha}$

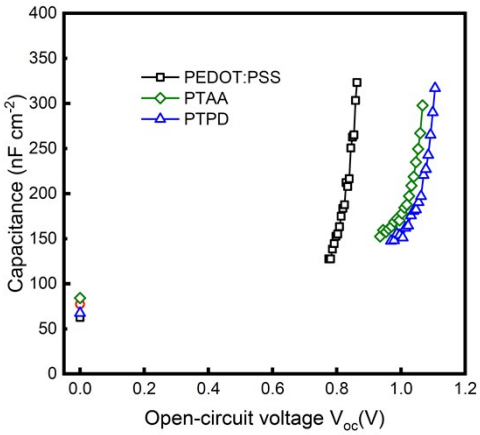

Figure S7 Device capacitance as a function of V_{OC}.

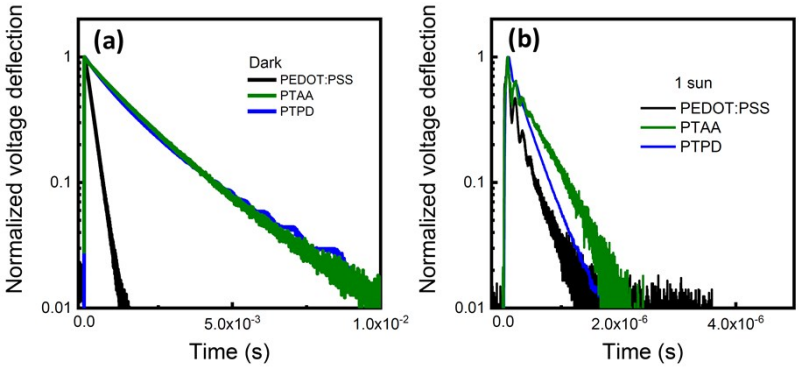

Figure S8 Decay of transient photovoltage at two representative light intensities: dark and 1-Sun. A rate constant can be extracted by fitting these mono-exponential decay.

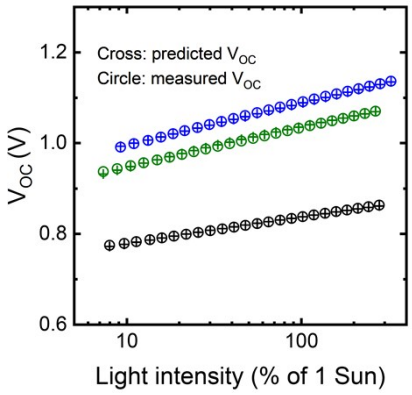

Figure S9 Measured V_{OC} (crosses) vs reconstructed V_{OC} (circles) of the solar cells with various HTLs.

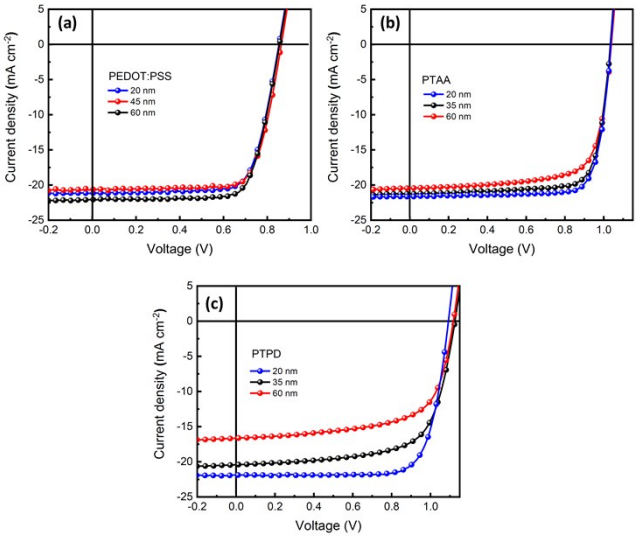

Figure S10 J-V characteristics of solar cells based on PEDOT:PSS, PTAA and PTPD with varied HTL thickness

Table S1 Energetics of HTLs and ITO.

	PEDOT:PSS	PTPD*	PTAA*	ITO
Work function (eV)	5.007 ± 0.008	4.686 ± 0.003 (4.817 ± 0.002)	4.740 ± 0.001 (4.851 ± 0.001)	5.101 ± 0.002
Ionization potential (eV)	5.116 ± 0.012	5.084 ± 0.007	5.015 ± 0.011	--

*The work function is measured with a thin PFN layer on top as surface compatibilizer.

Table S2 (110) diffraction peak parameters of MAPI films on different HTLs.

	PEDOT:PSS	PTPD	PTAA
Peak position (degree)	14.15	14.16	14.14
FWHM (degree)	0.10	0.10	0.09
Peak intensity (count)	16567	16264	15386

Table S3 Series and shunt resistance of the solar cells based on various HTLs.

	PEDOT:PSS	PTPD	PTAA
R_{sh} (Ohm cm^2)	(1.56 ± 0.02) x 10^3	(2.93 ± 0.03) x 10^4	(3.75 ± 0.02) x 10^4
R_s(Ohm cm^2)	4.35 ± 0.11	5.22 ± 0.05	4.32 ± 0.06